

PHD Extended Target Tracking Using an Incoherent X-band Radar: Preliminary Real-World Experimental Results

Karl Granström*, Antonio Natale†, Paolo Braca‡, Giovanni Ludeno† and Francesco Serafino†

*Department of Electrical Engineering, Linköping University, Linköping, Sweden. Email: karl@isy.liu.se

†IREA-CNR, Napoli, Italy. Email: {natale.a, ludeno.g, serafino.f}@irea.cnr.it

‡NATO STO CMRE, La Spezia, Italy. Email: braca@cmre.nato.int

Abstract—X-band radar systems represent a flexible and low-cost tool for ship detection and tracking. These systems suffer the interference of the sea-clutter but at the same time they can provide high measurement resolutions, both in space and time. Such features offer the opportunity to get accurate information about the target’s state and shape. Accordingly, here we exploit an extended target tracking methodology based on the popular Probability Hypothesis Density to get information about the targets observed in an actual X-band radar dataset. For each target track we estimate the target’s position, velocity and acceleration, as well as its size and the expected number of radar returns.

Index Terms—Multiple target tracking, GGIW-PHD, X-band radar, extended targets, real-world experimental results

I. MOTIVATION AND RELATED WORKS

X-band radar systems represent an useful tool for many civil and military applications, including weather monitoring, air traffic control and maritime vessel traffic control. Besides, the smart processing of data provided by such systems allows us to get useful information about the parameters characterizing the wave motion as well as to retrieve surface currents and bathymetry maps [1]–[3]. Therefore, these devices are arousing increasing interest in last decade: indeed, thanks to their operative flexibility, comparatively limited costs and easiness of installation, they result to be particularly suitable to scan the sea surface with high temporal and spatial resolution on fixed, moving and - if need be - opportunity platforms.

However, in spite of their versatility, incoherent X-band radars are mostly employed for high resolution surveillance purposes but, in these scenarios, they cannot be considered as reliable as coherent systems in terms of target detection capabilities. Accordingly, the employment of an effective tracking strategy can play a fundamental role in these circumstances, leading to a significant improvement in the surveillance performances provided by such systems.

Among the several emerging target tracking methodologies one of the most promising is the Probability Hypothesis Density (PHD) filter [4]. Indeed, in [5], [6] authors have proven that the multi-sensor PHD function behaves, by increasing the number of sensors, as a mixture of as many Gaussian components as the true number of targets. These Gaussian functions become progressively narrower and peakier around

the true target states in a way that is ruled by the Fisher information [6]. In other words, the PHD is asymptotically optimal increasing the number of sensors. The PHD is suitable to deal with a cluttered environment and with appearing/disappearing moving targets without using track-management logics.

In the present work we deal with high resolution radar images or, in other words, with *extended* targets. Typically, in the target tracking applications, a target gives rise to at most one measurement per time step and then the point-wise target assumption is commonly adopted and well-accepted, see e.g. [7]. However, in many applications a target can potentially give rise to more than one measurement per time step, leading to the problem of extended target, see e.g. [8]. Given the nature of marine X-band radars, the measurements are such that there are multiple detections per target. The number of detections caused by a target per time step is modeled as Poisson distributed [9], [10]. There are many different models for the extended targets extension, i.e. the representation of its size and shape. In this work we have used the random matrix model [11], [12], which means that the size of an extended target is approximated by an ellipse.

Previously extended target tracking models have been applied to laser range data, see e.g. [8], [13]–[18], Kinect data, see e.g. [19], and video data, see e.g. [20]. Track-before-detect of single extended targets can be found in [21], [22]. In this work we present a gamma Gaussian inverse Wishart (GGIW) implementation of the extended target PHD filter [23] to process a dataset acquired in October 2013 by a marine X-band radar mounted in Tuscany (Italy). The detected targets occupy several of the sensor’s resolution cells and are thus extended. To the best of our knowledge, this is the first time algorithms for multiple extended target tracking are applied to X-band radar data.

II. THE GGIW-PHD FILTER FOR MULTIPLE EXTENDED TARGET TRACKING

The measurements were used as input in a gamma-Gaussian-inverse Wishart (GGIW) implementation of the extended target PHD filter presented in [23]. The GGIW-PHD filter is an extension of the GIW-PHD filter presented in [14], [24], where measurement rate estimation has been added as outlined

TABLE I
NOTATION

- \mathbb{R}^n is the set of real n -vectors, \mathbb{S}_+^n is the set of symmetric positive semi-definite $n \times n$ -matrices, and \mathbb{S}_{++}^n is the set of symmetric positive definite $n \times n$ -matrices.
- $\mathcal{G}(\gamma; \alpha, \beta)$ denotes a gamma probability density function (pdf) defined over the scalar $\gamma > 0$ with scalar shape parameter $\alpha > 0$ and scalar inverse scale parameter $\beta > 0$,

$$\mathcal{G}(\gamma; \alpha, \beta) = \beta^\alpha \Gamma(\alpha)^{-1} \gamma^{\alpha-1} e^{-\beta\gamma}, \quad (1)$$

where $\Gamma(\cdot)$ is the gamma function.

- $\mathcal{N}(x; m, P)$ denotes the probability density function (pdf) of a Gaussian distribution defined over the vector x , with mean vector $m \in \mathbb{R}^n$ and covariance matrix $P \in \mathbb{S}_+^n$.

- $\mathcal{IW}_d(X; v, V)$ denotes an inverse Wishart pdf defined over the matrix $X \in \mathbb{S}_{++}^d$ with scalar degrees of freedom $v > 2d$ and parameter matrix $V \in \mathbb{S}_{++}^d$, [26, Definition 3.4.1]

$$\mathcal{IW}_d(X; v, V) = \frac{2^{-\frac{v-d-1}{2}} \det(V)^{\frac{v-d-1}{2}}}{\Gamma_d\left(\frac{v-d-1}{2}\right) \det(X)^{\frac{v}{2}}} \text{etr}\left(-\frac{1}{2}X^{-1}V\right), \quad (2)$$

where $\text{etr}(\cdot) = \exp(\text{Tr}(\cdot))$ is exponential of the matrix trace, and $\Gamma_d(\cdot)$ is the multivariate gamma function. The multivariate gamma function $\Gamma_d(\cdot)$ can be expressed as a product of the ordinary gamma function $\Gamma(\cdot)$, see [26, Theorem 1.4.1].

- $\mathbf{Z}^k = \left\{ \mathbf{z}_k^{(j)} \right\}_{j=1}^{N_{z,k}}$ is a measurement set at time t_k , where $\mathbf{z}_k^{(j)} \in \mathbb{R}^{n_z}$, $\forall j$. \mathbf{Z}^k denotes all measurement sets from time t_0 to time t_k .

- $V(\mathcal{A})$ is the volume of the surveillance area, $\lambda_k \triangleq \beta_{FA,k} V(\mathcal{A})$ is the mean number of clutter measurements and $c_k(\mathbf{z}_k) = 1/V(\mathcal{A})$ is the spatial distribution of the clutter over the surveillance volume.

- $\mathcal{P}\mathcal{Z}$ denotes all the partitions \mathcal{P} of the set \mathbf{Z} . A partition \mathcal{P} is a set of non-empty subsets \mathbf{W} called cells. The union of all cells \mathbf{W} is equal to the set \mathbf{Z} . The cardinality of a cell \mathbf{W} is denoted $|\mathbf{W}|$.

- For each cell \mathbf{W} in each partition \mathcal{P} the centroid measurement and scatter matrix are defined as

$$\bar{\mathbf{z}}_k^{\mathbf{W}} = \frac{1}{|\mathbf{W}|} \sum_{\mathbf{z}_k^{(i)} \in \mathbf{W}} \mathbf{z}_k^{(i)}, \quad (3a)$$

$$\mathbf{Z}_k^{\mathbf{W}} = \sum_{\mathbf{z}_k^{(i)} \in \mathbf{W}} \left(\mathbf{z}_k^{(i)} - \bar{\mathbf{z}}_k^{\mathbf{W}} \right) \left(\mathbf{z}_k^{(i)} - \bar{\mathbf{z}}_k^{\mathbf{W}} \right)^T. \quad (3b)$$

- $f[g]$ denotes the integral $\int f(x)g(x)dx$.
- $\delta_{i,j}$ is the Kronecker delta, and \otimes is the Kronecker product.
- \mathbf{I}_n is a $n \times n$ identity matrix and $\mathbf{0}_{m \times n}$ is an $m \times n$ all zero matrix.

in [25]. The derivation details are omitted due to page limits, the notation is presented in Table I.

A. Models

The extended target state ξ_k is defined as the triple

$$\xi_k \triangleq (\gamma_k, \mathbf{x}_k, X_k). \quad (4)$$

Here the random vector $\mathbf{x}_k = [\mathbf{p}_k, \mathbf{v}_k, \mathbf{a}_k]^T \in \mathbb{R}^{n_x}$ is the kinematical state, and describes the target's position $\mathbf{p}_k \in \mathbb{R}^d$, velocity $\mathbf{v}_k \in \mathbb{R}^d$ and acceleration $\mathbf{a}_k \in \mathbb{R}^d$. The random matrix $X_k \in \mathbb{S}_{++}^d$ is the extension state and describes the target's size and shape. Under the random matrix model [11], [12] the target shape is assumed to be an ellipse. Lastly, the random variable $\gamma_k > 0$ is the measurement rate that describes how many measurements the target, on average, generates per time step. In this paper the number of target generated measurements is assumed to be Poisson distributed, and γ_k is in this case the Poisson rate.

Conditioned on a history of previous measurement sets, denoted \mathbf{Z}^k , the extended target state ξ_k is modeled as being gamma-Gaussian-inverse Wishart distributed [11], [25],

$$\begin{aligned} p(\xi_k | \mathbf{Z}^k) &= p(\gamma_k | \mathbf{Z}^k) p(\mathbf{x}_k | X_k, \mathbf{Z}^k) p(X_k | \mathbf{Z}^k) \\ &= \mathcal{G}(\gamma_k; \alpha_{k|k}, \beta_{k|k}) \mathcal{N}(\mathbf{x}_k; m_{k|k}, P_{k|k} \otimes X_k) \\ &\quad \times \mathcal{IW}_d(X_k; v_{k|k}, V_{k|k}). \end{aligned} \quad (5a) \quad (5b)$$

We also use the short hand notation

$$p(\xi_k | \mathbf{Z}^k) = \mathcal{GGIW}(\xi_k; \zeta_{k|k}), \quad (6)$$

where $\zeta_{k|k} = \{\alpha_{k|k}, \beta_{k|k}, m_{k|k}, P_{k|k}, v_{k|k}, V_{k|k}\}$ is the set of GGIW density parameters.

Note that (5) assumes that the measurement rate is independent of the kinematic and extension states. In reality the number of measurements that a target generates is typically dependent on the size of the target and the distance between the target and the sensor (i.e. dependent on the target's position), where a larger and/or closer target typically generates more measurements compared to a more smaller and/or more distant target. However, modelling this dependence is not easy in the general case, and it has been shown in simulations that the assumption does not restrict the estimation performance, see e.g. [25], [27].

Both the measurement rate and the extension state are assumed to be approximately constant over time. For the kinematics state we use the dynamical model [11]

$$\mathbf{x}_{k+1} = (F_{k+1|k} \otimes \mathbf{I}_d) \mathbf{x}_k + \mathbf{w}_{k+1}, \quad (7)$$

where \mathbf{w}_{k+1} is zero mean Gaussian process noise with covariance $\Delta_{k+1|k} = \mathbf{Q}_{k+1|k} \otimes X_{k+1}$. $F_{k+1|k}$ and $\mathbf{Q}_{k+1|k}$ are [11]

$$F_{k+1|k} = \begin{bmatrix} 1 & T_s & \frac{1}{2}T_s^2 \\ 0 & 1 & T_s \\ 0 & 0 & e^{-T_s/\theta} \end{bmatrix}, \quad (8a)$$

$$\mathbf{Q}_{k+1|k} = \Sigma^2 \left(1 - e^{-2T_s/\theta} \right) \text{diag}([0 \ 0 \ 1]), \quad (8b)$$

where T_s is the sampling time, Σ is the scalar acceleration standard deviation and θ is the maneuver correlation time. The measurement rate and extension state are assumed to be approximately constant over time, i.e.,

$$\gamma_{k+1} \approx \gamma_k, \quad X_{k+1} \approx X_k \quad (9)$$

See [11], [12], [28] for longer discussions on dynamics modeling for the extension state. In this work it was not necessary to model rotation of the extension, which typically happens during a turning maneuver. Refer to [28] for a motion model that allows for kinematic state dependent rotations of the extension.

The number of target generated measurements is a random variable that is assumed to be Poisson distributed with rate γ_k . The effective probability of detection for a target is [23]

$$P_{k,D}^e = (1 - e^{-\gamma_k}) P_D \quad (10)$$

where $P_D \in [0, 1]$. The measurement model is [11]

$$\mathbf{z}_k = (H_k \otimes \mathbf{I}_d) \mathbf{x}_k + \mathbf{e}_k, \quad (11)$$

where $H_k = [1 \ 0 \ 0]$ and \mathbf{e}_k is zero mean Gaussian noise with covariance given by the target extension matrix X_k .

B. Time update

Let the PHD intensity $D_{k|k}(\cdot)$ at time t_k , given measurement sets up to and including time t_k , be a mixture of GGIW distributions,

$$D_{k|k}(\xi_k) = \sum_{j=1}^{J_{k|k}} w_{k|k}^{(j)} \mathcal{GGIW}(\xi_k; \zeta_{k|k}^{(j)}), \quad (12)$$

where $J_{k|k}$ is the number of components, $w_{k|k}^{(j)}$ is the weight of the j th component, and $\zeta_{k|k}^{(j)}$ is the density parameter of the j th component. The predicted PHD intensity is a GGIW mixture,

$$D_{k+1|k}(\xi_{k+1}) = D_{k+1}^b(\xi_{k+1}) + D_{k+1}^s(\xi_{k+1}), \quad (13)$$

with two parts corresponding to new targets and surviving existing targets. In this work models for target spawning were not necessary and were thus omitted. Refer to [29] for spawning modeling within the random matrix extended target model.

1) *New targets*: In previous work on multiple extended target tracking using PHD filter the birth intensities have been modeled as distribution mixtures, where each mixture component corresponds to a location where it is likely that new targets will appear. In the data set used in this paper it is not known a priori where the targets are likely to appear, instead new targets may appear anywhere in the surveillance area. Following the work in [30], [31] we use the following intensity for the birth PHD,

$$\begin{aligned} D_k^b(\xi_k) &= w_k^{(b)} \mathcal{U}(\mathbf{p}_k) \mathcal{N}([\mathbf{v}_k, \mathbf{a}_k]^\top; m_k^{(b)}, P_k^{(b)} \otimes X_k) \\ &\times \mathcal{G}(\gamma_k; \alpha_k^{(b)}, \beta_k^{(b)}) \mathcal{IW}_d(X_k; v_k^{(b)}, V_k^{(b)}). \end{aligned} \quad (14)$$

The birth measurement rate and extension are modeled as gamma and inverse Wishart distributed. The velocity and acceleration are modeled as Gaussian distributed, however for the birth position a uniform distribution over the surveillance area is used.

2) *Surviving existing targets*: The PHD intensity corresponding to existing targets that remain in the surveillance area is

$$D_{k+1|k}^s(\xi_{k+1}) = \sum_{j=1}^{J_{k|k}} w_{k+1|k}^{(j)} \mathcal{GGIW}(\xi_{k+1}; \zeta_{k+1|k}^{(j)}), \quad (15a)$$

$$w_{k+1|k}^{(j)} = P_S w_{k|k}^{(j)} \quad (15b)$$

$$\alpha_{k+1|k}^{(j)} = \frac{\alpha_{k|k}^{(j)}}{\eta_k}, \quad \beta_{k+1|k}^{(j)} = \frac{\beta_{k|k}^{(j)}}{\eta_k}, \quad (15c)$$

$$m_{k+1|k}^{(j)} = (F_{k+1|k} \otimes \mathbf{I}_d) m_{k|k}^{(j)}, \quad (15d)$$

$$P_{k+1|k}^{(j)} = F_{k+1|k} P_{k|k}^{(j)} F_{k+1|k}^\top + \mathbf{Q}_{k+1|k}, \quad (15e)$$

$$v_{k+1|k}^{(j)} = 2d + 2 + e^{-T_s/\tau} (v_{k|k}^{(j)} - 2d - 2), \quad (15f)$$

$$V_{k+1|k}^{(j)} = \frac{v_{k+1|k}^{(j)} - 2d - 2}{v_{k|k}^{(j)} - 2d - 2} V_{k|k}^{(j)}. \quad (15g)$$

For the kinematical state \mathbf{x}_k the prediction follows from the motion model (8). For the measurement rate the expected value is kept constant, and the variance is increased by multiplying with a factor η_k . The extension state's expected value is also kept constant, while the degrees of freedom are decreased corresponding to an increased variance.

C. Measurement update

Let the predicted PHD intensity at time t_k be

$$D_{k|k-1}(\xi_k) = D_k^b(\xi_k) + \sum_{j=1}^{J_{k|k-1}} w_{k|k-1}^{(j)} \mathcal{GGIW}(\xi_k; \zeta_{k|k-1}^{(j)}). \quad (16)$$

The measurement update is [23]

$$D_{k|k}(\xi_k | \mathbf{Z}^k) = L_{\mathbf{z}_k}(\xi_k) D_{k|k-1}(\xi_k | \mathbf{Z}^{k-1}). \quad (17)$$

The measurement pseudo-likelihood function $L_{\mathbf{z}_k}(\cdot)$ in (17) is defined as

$$\begin{aligned} L_{\mathbf{z}_k}(\xi_k) &\triangleq 1 - P_{k,D}^e + \\ &e^{-\gamma_k} P_D \sum_{\mathcal{P} \subseteq \mathbf{Z}_k} \omega_{\mathcal{P}} \sum_{\mathbf{W} \in \mathcal{P}} \frac{\gamma_k^{|\mathbf{W}|}}{d_{\mathbf{W}}} \prod_{\mathbf{z}_k \in \mathbf{W}} \frac{\phi_{\mathbf{z}_k}(\xi_k)}{\lambda_k c_k(\mathbf{z}_k)}, \end{aligned} \quad (18)$$

where

- the first part corresponds to missed detections, and the second part corresponds to detected targets;
- the quantities $\omega_{\mathcal{P}}$ and $d_{\mathbf{W}}$ are non-negative coefficients defined, for each partition \mathcal{P} and cell \mathbf{W} respectively, as

$$\omega_{\mathcal{P}} = \frac{\prod_{\mathbf{W} \in \mathcal{P}} d_{\mathbf{W}}}{\sum_{\mathcal{P}' \subseteq \mathbf{Z}_k} \prod_{\mathbf{W}' \in \mathcal{P}'} d_{\mathbf{W}'}} \quad (19)$$

$$d_{\mathbf{W}} = \delta_{|\mathbf{W}|,1} + D_{k|k-1} \left[P_D \gamma_k^{|\mathbf{W}|} e^{-\gamma_k} \prod_{\mathbf{z}_k \in \mathbf{W}} \frac{\phi_{\mathbf{z}_k}(\cdot)}{\lambda_k c_k(\mathbf{z}_k)} \right]. \quad (20)$$

- $\phi_{\mathbf{z}_k}(\xi_k) \triangleq p(\mathbf{z}_k | \xi_k)$ is the likelihood function for a single target generated measurement. Under the measurement model (11) it is given as

$$\phi_{\mathbf{z}_k}(\xi_k) = \mathcal{N}(\mathbf{z}_k; (H_k \otimes \mathbf{I}_d) \mathbf{x}_k, X_k). \quad (21)$$

For Bayes optimality the measurement update should consider all possible partitions \mathcal{P} of the measurement set \mathbf{Z}_k , but this is not computationally tractable in practice [8], [14], [32]. In this work we have used the methods from [8], [14] to compute a subset of partitions. The posterior PHD is a GGIW mixture,

$$D_{k|k}(\xi_k) = D_{k|k}^m(\xi_k) + D_{k|k}^b(\xi_k) + D_{k|k}^d(\xi_k), \quad (22)$$

with three parts corresponding to not detected previously existing targets, new targets, and detected previously existing targets.

1) *Not detected previously existing targets*: Following [30], [31], it is assumed that when a new target appears it always generates at least one measurement in the first time step it exists. This corresponds to the effective probability of detection being unity, $P_{k,D}^e = 1$. Therefore we only consider missed detections for previously existing targets. The updated PHD corresponding to previously existing targets that are not detected is

$$D_{k|k}^m(\xi_k) = \sum_{j=1}^{J_{k|k-1}} (1 - P_{k,D}^e) w_{k|k-1}^{(j)} \mathcal{G}\mathcal{G}\mathcal{I}\mathcal{W}(\xi_k; \zeta_{k|k-1}^{(j)}) \quad (23)$$

$$= \sum_{j=1}^{J_{k|k-1}} p^{(j)}(\gamma_k) \mathcal{N}(\mathbf{x}_k; m_{k|k}^{(j)}, P_{k|k}^{(j)} \otimes X_k) \times \mathcal{I}\mathcal{W}_d(X_k; v_{k|k}^{(j)}, V_{k|k}^{(j)}) \quad (24)$$

where $p^{(j)}(\gamma_k)$ is

$$p^{(j)}(\gamma_k) = (1 - P_D) w_{k|k-1}^{(j)} \mathcal{G}(\gamma_k; \alpha_{k|k}^{(j)}, \beta_{k|k}^{(j)}) + P_D \left(\frac{\beta_{k|k}^{(j)}}{\beta_{k|k}^{(j)} + 1} \right)^{\alpha_{k|k}^{(j)}} w_{k|k-1}^{(j)} \mathcal{G}(\gamma_k; \alpha_{k|k}^{(j)}, \beta_{k|k}^{(j)} + 1). \quad (25)$$

Using gamma-mixture reduction, see [25], $p^{(j)}(\gamma_k)$ is approximated as

$$\tilde{p}^{(j)}(\gamma_k) = \tilde{w}_{k|k}^{(j)} \mathcal{G}(\gamma_k; \tilde{\alpha}_{k|k}^{(j)}, \tilde{\beta}_{k|k}^{(j)}). \quad (26)$$

This gives the PHD intensity approximation

$$D_{k|k}^m(\xi_k) \approx \sum_{j=1}^{J_{k|k-1}} \tilde{w}_{k|k}^{(j)} \mathcal{G}\mathcal{G}\mathcal{I}\mathcal{W}(\xi_k; \tilde{\zeta}_{k|k}^{(j)}), \quad (27)$$

where $\tilde{\zeta}_{k|k}^{(j)} = \{\tilde{\alpha}_{k|k}^{(j)}, \tilde{\beta}_{k|k}^{(j)}, m_{k|k-1}^{(j)}, P_{k|k-1}^{(j)}, v_{k|k-1}^{(j)}, V_{k|k-1}^{(j)}\}$.

2) *New targets*: The updated PHD corresponding to new targets is

$$D_{k|k}^b(\xi_k) = \sum_{\mathcal{P} \setminus \mathcal{Z}_k} \sum_{\mathbf{W} \in \mathcal{P}} w_{k|k}^{(b, \mathbf{W})} \mathcal{G}\mathcal{G}\mathcal{I}\mathcal{W}(\xi_k; \zeta_{k|k}^{(b, \mathbf{W})}), \quad (28)$$

where

$$\alpha_{k|k}^{(b, \mathbf{W})} = \alpha_k^{(b)} + |\mathbf{W}|, \quad \beta_{k|k}^{(b, \mathbf{W})} = \beta_k^{(b)} + 1, \quad (29a)$$

$$m_{k|k}^{(b, \mathbf{W})} = \left[(\bar{z}_k^{\mathbf{W}})^{\top}, \left(m_k^{(b)} \right)^{\top} \right]^{\top}, \quad (29b)$$

$$P_{k|k}^{(b, \mathbf{W})} = \text{blkdiag} \left(|\mathbf{W}|^{-1}, P_k^{(b)} \right), \quad (29c)$$

$$v_{k|k}^{(b, \mathbf{W})} = v_{k|k-1}^{(b)} + |\mathbf{W}|, \quad V_{k|k}^{(b, \mathbf{W})} = V_{k|k-1}^{(b)} + Z_k^{\mathbf{W}}. \quad (29d)$$

The updated position is Gaussian distributed with mean equal to the centroid measurement. This update is approximate, but as shown in [30], [31], the approximation can be justified as long as most of the probability mass of the likelihood is contained inside the surveillance area.

3) *Detected previously existing targets*: The updated PHD corresponding to detected previously existing targets is

$$D_{k|k}^d(\xi_k) = \sum_{\mathcal{P} \setminus \mathcal{Z}_k} \sum_{\mathbf{W} \in \mathcal{P}} \sum_{j=1}^{J_{k|k-1}} w_{k|k}^{(j, \mathbf{W})} \mathcal{G}\mathcal{G}\mathcal{I}\mathcal{W}(\xi_k; \zeta_{k|k}^{(j, \mathbf{W})}), \quad (30)$$

where

$$\alpha_{k|k}^{(j, \mathbf{W})} = \alpha_{k|k-1}^{(j)} + |\mathbf{W}|, \quad \beta_{k|k}^{(j, \mathbf{W})} = \beta_{k|k-1}^{(j)} + 1, \quad (31a)$$

$$m_{k|k}^{(j, \mathbf{W})} = m_{k|k-1}^{(j)} + \left(K_{k|k-1}^{(j, \mathbf{W})} \otimes \mathbf{I}_d \right) \varepsilon_{k|k-1}^{(j, \mathbf{W})}, \quad (31b)$$

$$P_{k|k}^{(j, \mathbf{W})} = P_{k|k-1}^{(j)} - K_{k|k-1}^{(j, \mathbf{W})} S_{k|k-1}^{(j, \mathbf{W})} \left(K_{k|k-1}^{(j, \mathbf{W})} \right)^{\top}, \quad (31c)$$

$$v_{k|k}^{(j, \mathbf{W})} = v_{k|k-1}^{(j)} + |\mathbf{W}|, \quad (31d)$$

$$V_{k|k}^{(j, \mathbf{W})} = V_{k|k-1}^{(j)} + N_{k|k-1}^{(j, \mathbf{W})} + Z_k^{\mathbf{W}}, \quad (31e)$$

and the innovation factor, gain vector, innovation vector and innovation matrix are

$$S_{k|k-1}^{(j, \mathbf{W})} = H_k P_{k|k-1}^{(j)} H_k^{\top} + |\mathbf{W}|^{-1} \quad (31f)$$

$$K_{k|k-1}^{(j, \mathbf{W})} = P_{k|k-1}^{(j)} H_k^{\top} \left(S_{k|k-1}^{(j, \mathbf{W})} \right)^{-1} \quad (31g)$$

$$\varepsilon_{k|k-1}^{(j, \mathbf{W})} = \bar{z}_k^{\mathbf{W}} - (H_k \otimes \mathbf{I}_d) m_{k|k-1}^{(j)} \quad (31h)$$

$$N_{k|k-1}^{(j, \mathbf{W})} = \left(S_{k|k-1}^{(j, \mathbf{W})} \right)^{-1} \varepsilon_{k|k-1}^{(j, \mathbf{W})} \left(\varepsilon_{k|k-1}^{(j, \mathbf{W})} \right)^{\top} \quad (31i)$$

4) *Weights*: The weights of the GGIW components corresponding to detected targets are

$$w_{k|k}^{(b, \mathbf{W})} = \frac{\omega_{\mathcal{P}} \mathcal{L}_k^{(b, \mathbf{W})} w_k^{(b)}}{d_{\mathbf{W}} \beta_{FA,k}^{|\mathbf{W}|} V(\mathcal{A})} \quad (32a)$$

$$w_{k|k}^{(j, \mathbf{W})} = \frac{\omega_{\mathcal{P}} P_D \mathcal{L}_k^{(j, \mathbf{W})} w_{k|k-1}^{(j)}}{d_{\mathbf{W}} \beta_{FA,k}^{|\mathbf{W}|}}, \quad (32b)$$

where

$$d_{\mathbf{W}} = \delta_{|\mathbf{W}|,1} + \frac{\mathcal{L}_k^{(b, \mathbf{W})} w_k^{(b)}}{\beta_{FA,k}^{|\mathbf{W}|} V(\mathcal{A})} + \sum_{j=1}^{J_{k|k-1}} \frac{P_D \mathcal{L}_k^{(j, \mathbf{W})} w_{k|k-1}^{(j)}}{\beta_{FA,k}^{|\mathbf{W}|}} \quad (32c)$$

$$\mathcal{L}_k^{(b, \mathbf{W})} = \frac{|\mathbf{W}|^{-d/2}}{\pi^{|\mathbf{W}|(d-1)/2}} \frac{\Gamma_d \left(\frac{v_{k|k}^{(b, \mathbf{W})}}{2} \right) \left| V_k^{(b)} \right|^{\frac{v_k^{(b)} - d - 1}{2}}}{\Gamma_d \left(\frac{v_k^{(b)}}{2} \right) \left| V_{k|k}^{(b, \mathbf{W})} \right|^{\frac{v_{k|k}^{(b, \mathbf{W})} - d - 1}{2}}} \times \frac{\Gamma \left(\alpha_{k|k}^{(b, |\mathbf{W}|)} \right) \left(\beta_k^{(b)} \right)^{\alpha_k^{(b)}}}{\Gamma \left(\alpha_k^{(b)} \right) \left(\beta_{k|k}^{(b, \mathbf{W})} \right)^{\alpha_{k|k}^{(b, |\mathbf{W}|)}}} \quad (32d)$$

$$\mathcal{L}_k^{(j, \mathbf{W})} = \frac{(\pi^{|\mathbf{W}|} |\mathbf{W}|)^{-\frac{d}{2}} \left| V_{k|k-1}^{(j)} \right|^{\frac{v_{k|k-1}^{(j)}}{2}} \Gamma_d \left(\frac{v_{k|k-1}^{(j, \mathbf{W})}}{2} \right)}{\left(S_{k|k-1}^{(j, \mathbf{W})} \right)^{\frac{d}{2}} \left| V_{k|k}^{(j, \mathbf{W})} \right|^{\frac{v_{k|k}^{(j, \mathbf{W})}}{2}} \Gamma_d \left(\frac{v_{k|k}^{(j)} - 1}{2} \right)} \times \frac{\Gamma \left(\alpha_{k|k}^{(j, |\mathbf{W}|)} \right) \left(\beta_{k|k-1}^{(j)} \right)^{\alpha_{k|k-1}^{(j)}}}{\Gamma \left(\alpha_{k|k-1}^{(j)} \right) \left(\beta_{k|k}^{(j, \mathbf{W})} \right)^{\alpha_{k|k}^{(j, |\mathbf{W}|)}}} \quad (32e)$$

D. Extraction, maintenance and reduction

1) *Target extraction:* In each time step, a set of extracted targets is computed by taking the GGIW components for which $w_{k|k}^{(j)} > \bar{w}_0$,

$$\hat{\mathbf{X}}_{k|k} = \left\{ \hat{\xi}_{k|k}^{(i)} \right\}_{i:1}^{\hat{N}_{k|k}}, \quad (33)$$

$$\hat{\xi}_{k|k}^{(i)} = (\mathbb{E}[\gamma_k], \mathbb{E}[\mathbf{x}_k], \mathbb{E}[X_k]), \quad (34)$$

where the expected values are with respect to the GGIW component.

2) *Track maintenance:* To enable estimation of target tracks, similarly to [33], [34], a label scheme was utilized. Each GGIW component is associated to a label $\ell_{k|k}^{(j)}$ that is initialized as 0 upon new target birth. If the component is extracted, and a label has not yet been assigned (i.e. $\ell_{k|k}^{(j)} = 0$), a unique positive integer is assigned as label. In the time update and measurement update the predicted and corrected components are assigned the same label as the components from which they were updated. Label managing is performed in the mixture reduction step, see below.

A target track is considered confirmed if a GGIW component with an assigned label has been extracted for at least three consecutive time steps. The target track remains confirmed until the corresponding GGIW component is pruned from the PHD intensity. This procedure effectively minimizes the number of false target tracks, however it comes at the price of a delay in the confirmation of the tracks.

3) *Mixture reduction:* The number of components $J_{k|k}$ increases with time and must be reduced in each filter iteration. In a first step, all components for which either $w_{k|k}^{(j)} < T$, $\mathbb{E}[\gamma_k] = \alpha_{k|k}^{(j)} / \beta_{k|k}^{(j)} < 1$, or both, are pruned (i.e. discarded). Next, component merging is performed using modifications of the methods from [25], [35]:

- If $\ell_{k|k}^{(j)} = 0$ the component is not merged with any other component.
- Two components j and i are candidates for merging only if $\ell_{k|k}^{(j)} = \ell_{k|k}^{(i)}$ and the symmetric Kullback-Leibler divergence (KL-div) between the two components is less than U .
- Components are merged such that the weight $\tilde{w}_{k|k}^{(j)}$ is smaller than a threshold \bar{w}_1 .

After the merging label management is performed as follows. Let L be a set of GGIW components with identical

assigned labels. If

$$\max_{j \in L} w_{k|k}^{(j)} \geq \bar{w}_2 \vee \frac{\max_{j \in L} w_{k|k}^{(j)}}{\sum_{j \in L} w_{k|k}^{(j)}} > \bar{w}_3, \quad (35)$$

where \vee is logical or, then prune all components except the maximum weight one. Otherwise let the maximum weight component keep the assigned label and reset $\ell_{k|k}^{(j)} = 0$ for remaining components.

III. EXPERIMENTAL RESULTS

A. Description of the acquisition system

In order to assess the tracking performances of the GGIW-PHD filter, we consider the detections relevant to a set of actual data collected by an X-band incoherent radar. It is well known that these systems can represent a low-cost tool to detect targets with high temporal and spatial resolutions, even though they cannot be considered as reliable as coherent systems in terms of target detection capabilities. Nevertheless, an effective tracking strategy can play a crucial role to significantly improve their surveillance performances, especially with regard to the retrieval of the target's shape. In particular, here we exploit the dataset acquired on October 2013 by a coastal X-band radar mounted in Tuscany (Italy). The details of the acquisition system are given in Table II.

TABLE II
PARAMETERS OF THE ACQUISITION SYSTEM.

Parameter	Value
Antenna rotation period (Δt)	2.41 s
Range resolution (Δr)	7 m
Azimuth resolution ($\Delta \varphi$)	0.9°
Radar scale	3069 m
View angular sector	260°

B. Detection strategy

The raw data collected by the considered X-band radar have been processed by an Order Statistic-Constant False Alarm Rate (OS-CFAR) detector [36], [37].

The statistical analysis of the raw data led us to consider the Weibull distribution for the sea-clutter description (see Figure 1). Both the shape and scale parameter of the Weibull background have been estimated from each range-line of the raw data by exploiting the procedure shown in [38].

The retrieved value of these parameters allows us to completely define the Weibull clutter, whose knowledge is required to compute the local detection threshold [4]. The characteristic parameters of the employed OS-CFAR detector are listed in Table III.

TABLE III
PARAMETER SETTINGS OF THE OS-CFAR

Parameter	Value
False alarm probability (PFA)	10^{-9}
Samples of the Reference Window (M)	32(16 × 2)
Guard Cells (G)	8(4 × 2)
Representative rank of the noise level (k)	24(0.75M)

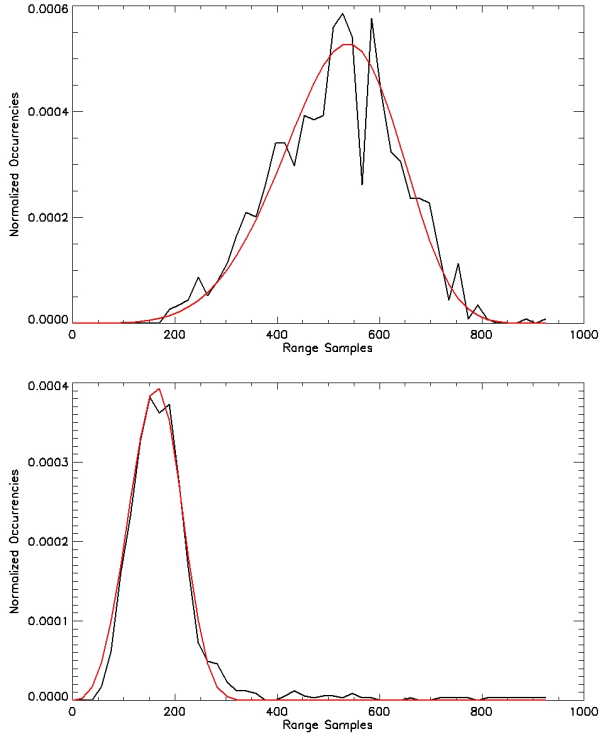


Fig. 1. A comparison of data histogram (black) and relevant Weibull distributions (red) for two different range lines.

TABLE IV
PARAMETER SETTINGS OF THE GGIW PHD FILTER

Parameter		Value
Probability of detection	P_D	0.99
Probability of survival	P_S	0.99
Clutter density	$\beta_{FA,k}$	$100/V(\mathcal{A})$
Sampling time	T_s	2.41
Rate forgetting factor	η_k	1.05
Acceleration st. dev.	Σ	1
Maneuver correlation time	θ	1
Temporal decay constant	τ	19.5
Birth weight	$w_k^{(b)}$	10^{-5}
Birth mean	$m_k^{(b)}$	$\mathbf{0}_{4 \times 1}$
Birth covariance	$P_k^{(b)}$	$10^{-2} I_2$
Birth measurement rate	$\alpha_k^{(b)}, \beta_k^{(b)}$	0.04, 0.008
Birth extension	$v_k^{(b)}, V_k^{(b)}$	12, $0.01 \mathbf{I}_d$
Extraction threshold	\bar{w}_0	0.5
Pruning threshold	T	10^{-3}
KL-div merging threshold	U	10
Merging weight thresholds	$\bar{w}_1, \bar{w}_2, \bar{w}_3$	1.1, 1, 0.8

C. Extended target tracker results

The X-band radar dataset considered here contains 30 radar scans. The GGIW PHD filter parameters that were used are given in Table IV. Before starting the tracking procedure, the detection results pertinent to each radar scan have been converted into Cartesian coordinates and then they have been provided to the GGIW-PHD filter. Figure 2 depicts a sample of the detector's output represented into Cartesian coordinates. Due to the high resolution of the acquisition system, in this

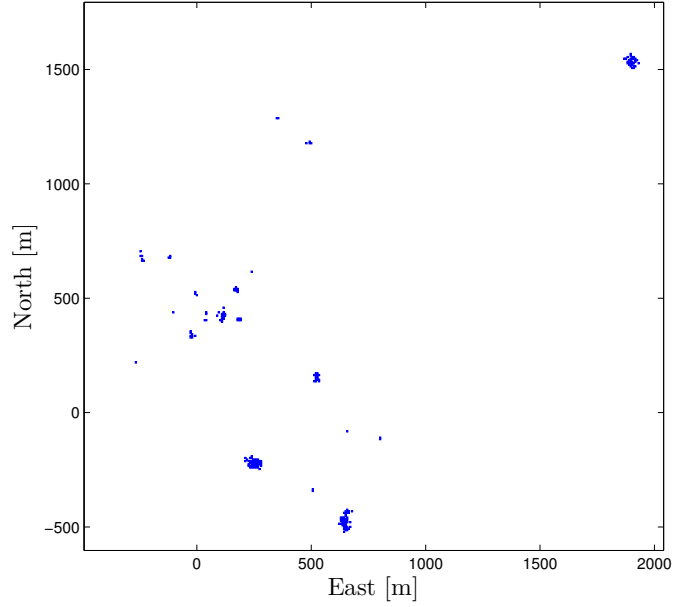


Fig. 2. Cartesian representation of detector's output relevant to a single radar scan. Sensor is located in origin.

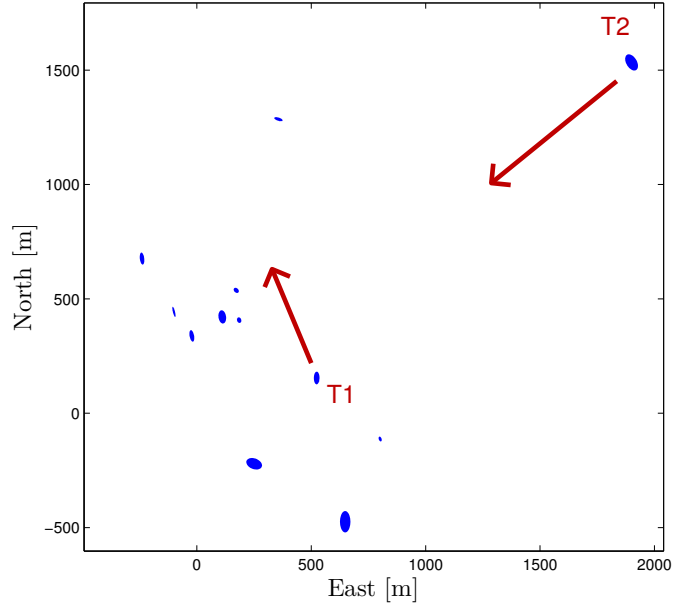


Fig. 3. Output of GGIW-PHD filter relevant to measurements depicted in Figure 2. Red arrows represent velocity directions of moving targets T1 and T2. Sensor is located in origin.

map each actual target is represented by a cluster of measurements. False alarms give rise to both punctual detections and small clusters.

Figure 3 shows the output from the GGIW-PHD filter corresponding to the detections in Figure 2. It is worth to note that during the acquisition of the considered dataset there were only two moving vessels (labeled as T1 and T2 in Figure 3) within the radar observation space. The remaining detection clusters depicted in Figure 2 are instead representative of steady targets

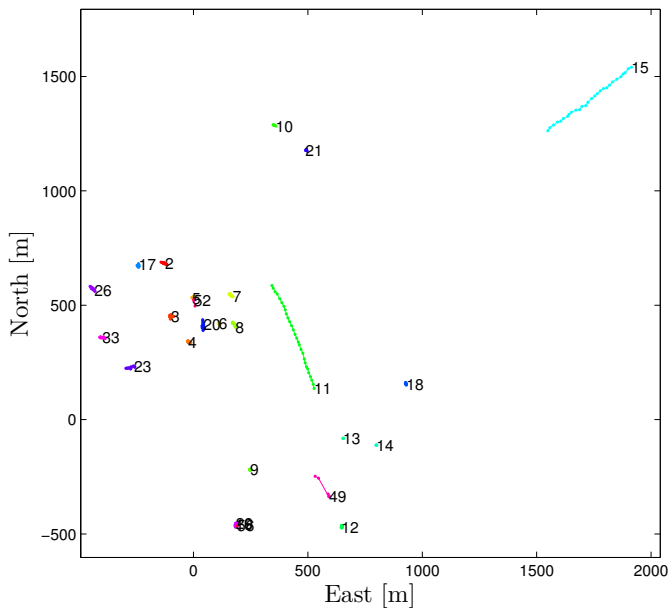


Fig. 4. Tracking history for GGIW PHD filter. Numbers indicate target label identities, and different colors are used for different target tracks. Target tracks T1 and T2 are assigned label identities 11 and 15, respectively.

like buoys, rocks and fixed boats.

As can be observed from a comparison between Figure 2 and Figure 3, the detection clusters (i.e., the actual targets) are properly mapped into ellipses during the tracking procedure. Recall that the shape of each ellipse results from using the random matrix extended target model [11]. The estimated positions of all confirmed target tracks are shown in Figure 4.

We also wish to highlight the GGIW-PHD filter’s robustness in retaining the dimensions of the extended targets over time. To give an idea of such capabilities, the tracks relevant to T1 and T2 acquired over the 30 scans are reported in Figure 5.

The computational times for the GGIW-PHD filter are given in Table V. The maximum time for a single filter cycle is less than 1.5 seconds, which is well under the antenna’s rotation period (2.41 seconds).

TABLE V
COMPUTATIONAL TIMES [MILLISECONDS]

Operation	Mean	St.dev.	Min	Max
Measurement set partitioning	175	75	60	291
Prediction and correction	542	239	24	1107
Mixture reduction	119	62	23	266
Extraction and maintenance	1.6	0.5	0.4	3.8
Total	837	319	116	1478

IV. CONCLUSIONS

Radar images acquired on October 2013 by a coastal incoherent X-band radar mounted in Tuscany (Italy) are processed using the GGIW implementation of the extended target PHD. Preliminary results have been reported, showing the capability of the proposed methodology to deal with interference of the sea-clutter and land and with multiple close-spaced targets

that appear and disappear in time. A GGIW-CPHD filter was presented in [27], in future work we intend to compare results for GGIW-PHD and GGIW-CPHD for the data.

ACKNOWLEDGMENT

Karl Granström would like to thank the project Collaborative Unmanned Aircraft Systems (CUAS), funded by the Swedish Foundation for Strategic Research (SSF), for financial support.

REFERENCES

- [1] J. Nieto Borge and C. Guedes Soares, “Analysis of directional wave fields using X-Band navigation radar,” *Coastal Engineering*, vol. 40, pp. 375–391, 2000.
- [2] G. Ludeno, A. Orlandi, C. Lugni, C. Brandini, F. Soldovieri, and F. Serafino, “X-band marine radar system for high-speed navigation purposes: A test case on a cruise ship,” *IEEE Geoscience and Remote Sensing Letters*, vol. 11, no. 1, pp. 244–248, 2014.
- [3] G. Ludeno, S. Flampouris, C. Lugni, F. Soldovieri, and F. Serafino, “A novel approach based on marine radar data analysis for high-resolution bathymetry map generation,” *IEEE Geoscience and Remote Sensing Letters*, vol. 11, no. 1, pp. 234–238, 2014.
- [4] N. Levanon and M. Shor, “Order statistics CFAR for weibull background,” *Proceedings of IEE...*, vol. 137, no. 3, Jun. 1990.
- [5] P. Braca, S. Marano, V. Matta, and P. Willett, “Multitarget-multisensor ml and phd: Some asymptotics,” in *Proceedings of the International Conference on Information Fusion*, Singapore, Jul. 2012.
- [6] —, “Asymptotic efficiency of the PHD in multitarget/multisensor estimation,” *IEEE Journal of Selected Topics in Signal Processing, Special Issue on Multi-target Tracking*, vol. 7, no. 3, pp. 553–564, Jun. 2013.
- [7] Y. Bar-Shalom, P. K. Willett, and X. Tian, *Tracking and data fusion, a handbook of algorithms*. YBS, 2011.
- [8] K. Granström, C. Lundquist, and U. Orguner, “Extended Target Tracking using a Gaussian Mixture PHD filter,” *IEEE Transactions on Aerospace and Electronic Systems*, vol. 48, no. 4, pp. 3268–3286, Oct. 2012.
- [9] K. Gilholm and D. Salmund, “Spatial distribution model for tracking extended objects,” *IEE Proceedings of Radar, Sonar and Navigation*, vol. 152, no. 5, pp. 364–371, Oct. 2005.
- [10] K. Gilholm, S. Godsill, S. Maskell, and D. Salmund, “Poisson models for extended target and group tracking,” in *Proceedings of Signal and Data Processing of Small Targets*, vol. 5913. San Diego, CA, USA: SPIE, Aug. 2005, pp. 230–241.
- [11] J. W. Koch, “Bayesian approach to extended object and cluster tracking using random matrices,” *IEEE Transactions on Aerospace and Electronic Systems*, vol. 44, no. 3, pp. 1042–1059, Jul. 2008.
- [12] M. Feldmann, D. Fränken, and J. W. Koch, “Tracking of extended objects and group targets using random matrices,” *IEEE Transactions on Signal Processing*, vol. 59, no. 4, pp. 1409–1420, Apr. 2011.
- [13] K. Granström, C. Lundquist, and U. Orguner, “Tracking Rectangular and Elliptical Extended Targets Using Laser Measurements,” in *Proceedings of the International Conference on Information Fusion*, Chicago, IL, USA, Jul. 2011, pp. 592–599.
- [14] K. Granström and U. Orguner, “A PHD filter for tracking multiple extended targets using random matrices,” *IEEE Transactions on Signal Processing*, vol. 60, no. 11, pp. 5657–5671, Nov. 2012.
- [15] S. Reuter and K. Dietmayer, “Pedestrian tracking using random finite sets,” in *Proceedings of the International Conference on Information Fusion*, Chicago, IL, USA, Jul. 2011, pp. 1101–1108.
- [16] M. Wieneke and W. Koch, “A PMHT approach for extended objects and object groups,” *IEEE Transactions on Aerospace and Electronic Systems*, vol. 48, no. 3, pp. 2349–2370, 2012.
- [17] K. Granström, S. Reuter, D. Meissner, and A. Scheel, “A multiple model PHD approach to tracking of cars under an assumed rectangular shape,” in *Proceedings of the International Conference on Information Fusion*, Salamanca, Spain, Jul. 2014.
- [18] A. Scheel, K. Granström, D. Meissner, S. Reuter, and K. Dietmayer, “Tracking and Data Segmentation Using a GGIW Filter with Mixture Clustering,” in *Proceedings of the International Conference on Information Fusion*, Salamanca, Spain, Jul. 2014.

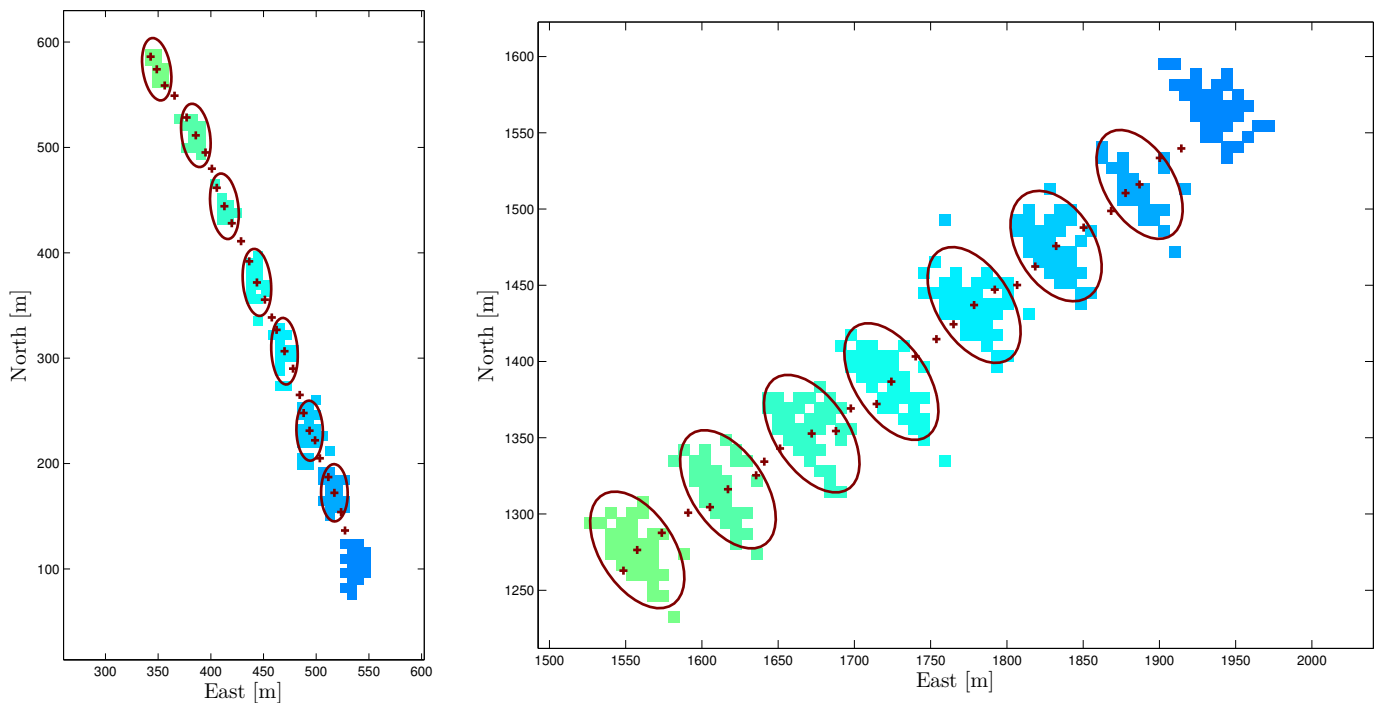


Fig. 5. Tracking history of extended targets T1 (left) and T2 (right). For each time step the estimated target position is shown as red crosses. For every fifth time step the detections are shown using color ranging from blue (first time step) to green (last time step), and the estimated extensions are shown as red ellipses. Note that only time steps for which the target tracks were confirmed are shown.

[19] M. Baum and U. D. Hanebeck, "Shape Tracking of Extended Objects and Group Targets with Star-Convex RHMs," in *Proceedings of the International Conference on Information Fusion*, Chicago, IL, USA, Jul. 2011, pp. 338–345.

[20] S. Davey, M. Wieneke, and H. Vu, "Histogram-PMHT unfettered," *IEEE Journal of Selected Topics in Signal Processing*, vol. 7, no. 3, pp. 435–447, June 2013.

[21] Y. Boers, H. Driessen, J. Torstensson, M. Trieb, R. Karlsson, and F. Gustafsson, "A track before detect algorithm for tracking extended targets," *IEE Proceedings Radar, Sonar and Navigation*, vol. 153, no. 4, pp. 345–351, Aug. 2006.

[22] B. Errasti-Alcala and P. Braca, "Track before detect algorithm for tracking extended targets applied to real-world data of x-band marine radar," in *Proceedings of the International Conference on Information Fusion*, Salamanca, Spain, Jul. 2014.

[23] R. Mahler, "PHD filters for nonstandard targets, I: Extended targets," in *Proceedings of the International Conference on Information Fusion*, Seattle, WA, USA, Jul. 2009, pp. 915–921.

[24] K. Granström and U. Orguner, "Implementation of the GIW-PHD filter," Department of Electrical Engineering, Linköping University, SE-581 83 Linköping, Sweden, Tech. Rep. LiTH-ISY-R-3046, Mar. 2012. [Online]. Available: <http://urn.kb.se/resolve?urn=urn:nbn:se:liu:diva-94585>

[25] —, "Estimation and Maintenance of Measurement Rates for Multiple Extended Target Tracking," in *Proceedings of the International Conference on Information Fusion*, Singapore, Jul. 2012, pp. 2170–2176.

[26] A. K. Gupta and D. K. Nagar, *Matrix variate distributions*, ser. Chapman & Hall/CRC monographs and surveys in pure and applied mathematics. Chapman & Hall, 2000.

[27] C. Lundquist, K. Granström, and U. Orguner, "An extended target CPHD filter and a gamma Gaussian inverse Wishart implementation," *IEEE Journal of Selected Topics in Signal Processing, Special Issue on Multi-target Tracking*, vol. 7, no. 3, pp. 472–483, Jun. 2013.

[28] K. Granström and U. Orguner, "A New Prediction Update for Extended Target Tracking with Random Matrices," *IEEE Transactions on Aerospace and Electronic Systems*.

[29] —, "On Spawning and Combination of Extended/Group Targets Modeled with Random Matrices," *IEEE Transactions on Signal Processing*, vol. 61, no. 3, pp. 678–692, Feb. 2013.

[30] M. Beard, B.-T. Vo, B.-N. Vo, and S. Arulampalam, "Gaussian Mixture PHD and CPHD Filtering with Partially Uniform Target Birth," in *Proceedings of the International Conference on Information Fusion*, Singapore, Jul. 2012, pp. 535–541.

[31] M. Beard, B. Vo, B.-N. Vo, and S. Arulampalam, "A partially uniform target birth model for gaussian mixture phd/cphd filtering," *IEEE Transactions on Aerospace and Electronic Systems*, vol. 49, no. 4, pp. 2835–2844, Oct. 2013.

[32] K. Granström, C. Lundquist, and U. Orguner, "A Gaussian mixture PHD filter for extended target tracking," in *Proceedings of the International Conference on Information Fusion*, Edinburgh, UK, Jul. 2010.

[33] D. E. Clark, K. Panta, and B.-N. Vo, "The GM-PHD Filter Multiple Target Tracker," in *Proceedings of the International Conference on Information Fusion*, Florence, Italy, Jul. 2006.

[34] K. Panta, D. Clark, and B.-N. Vo, "Data association and track management for the Gaussian mixture probability hypothesis density filter," *IEEE Transactions on Aerospace and Electronic Systems*, vol. 45, no. 3, pp. 1003–1016, Jul. 2009.

[35] K. Granström and U. Orguner, "On the Reduction of Gaussian inverse Wishart mixtures," in *Proceedings of the International Conference on Information Fusion*, Singapore, Jul. 2012, pp. 2162–2169.

[36] M. Skolnik, *Introduction to Radar Systems*. McGraw-Hill, 2002.

[37] N. Levanon, *Radar Principles*. Wiley & Co, 1988.

[38] S. D. Dubey, "Some percentile estimators for Weibull parameters," *Technometrics*, vol. 9, pp. 119–129, 1967.